DINAME 2017 - Proceedings of the XVII International Symposium on Dynamic Problems of Mechanics
A. T. Fleury, D. A. Rade, P. R. G. Kurka (Editors), ABCM, São Sebastião, SP, Brazil, March 5-10, 2017

Response analysis of bicycle model, 3 D.O.F. and multibody simulation compared with experiments on track and determination of their limits of utilization.

Roberto Bortolussi[1], **Jean Tavares Horcaio**[2]

[1] FEI University Center, roberto@fei.edu.br

[2] Ford Motor Company, jyzf@uol.com.br

Abstract: Simplified models are widely used in all areas of engineering with the purpose of estimating the responses of systems. In automotive engineering this is not different. However, knowing the limits of the use of a simplified model is crucial to guarantee correctness of the responses obtained with these models. The present work aims at explicitly deriving two different simplified mathematical models commonly used by the automotive community, and that sometimes are incorrectly derived, compare them with a multibody model correlated with a physical prototype on limit handling and steady state. This work will address the vehicle dynamics equations used for the mathematical modeling of two simplified models, bicycle model and three D.O.F. The equations were derived until the models are presented in state space. A multibody correlation with experimental test is described in this work. A graphical comparison shall be done based on yaw rate, lateral acceleration and rolling angle from the real vehicle responses versus a multibody model and versus both simplified models, verifying the differences between them. As a conclusion of this work, results differences was determined for the simplified models, different lateral acceleration from the usual 0.3 and 0.5 g, extensively used in papers that make use of these models.

Keywords: vehicle dynamics, CAE, 3 D.O.F. model, bicycle model, multibody model

NOMENCLATURE

Latin symbols

$\boldsymbol{v}$: tangential velocity
$\boldsymbol{m}$: vehicle mass
$\boldsymbol{m_s}$: sprung mass
$\boldsymbol{m_u}$: unsprung mass
$\boldsymbol{h_s}$: roll center distance to C.G.
$\boldsymbol{h_f}$: front roll center height
$\boldsymbol{h_r}$: rear roll center height
$\boldsymbol{l_f}$: distance from C.G. to front axel
$\boldsymbol{l_r}$: distance from C.G. to rear axel
$\boldsymbol{C_{sf}}$: front stick coefficient
$\boldsymbol{C_{sr}}$: rear stick coefficient
$\boldsymbol{I}$: inertia moment

Greek symbols

$\dot{\Psi}$: yaw rate
β : slip angle
δ : steering angle

Subscripts

x,y,z : relative to Cartesian coordinates

INTRODUCTION

The understanding the vehicle dynamic have been one challenge since the beginning of 20th century, when the automobile became one of most popular means of transportation. As described by Segel (1956), the dynamic vehicle studies can be divided in three parts. First period characterized by observations of dynamic behavior of the car, by vibrations on the steering wheel and recognizing the importance of the comfort inside the car. This first period is from the creation of the first car until the early 1930s. Then began a second period extending from the early 30's until the year of 1952. In this period started the formulation of the first models of two degrees of freedom in order to study the vehicle behavior during a curve and the first principles of vehicle dynamics were defined as, for example, tire slip angle and understeer and oversteer behavior. The third period started in 1952 and extends until nowadays. These years have been developed models with 3 DOF (degrees of freedom) and a tire model that enabled a greater understanding of tire behavior during acceleration, braking and curve. According Duarte (2010), the method of multibody systems was introduced in the automotive industry and gained strength from the 70's with the increase of computing resources. After this, a better

understanding of the vehicle's behavior was possible. Because of all this growth in knowledge of vehicle dynamics, studies relating to transient responses and directional stability began to be developed. In recent decades, in order to improve the safety of vehicle occupants, some controls systems was developed to help the driver avoid accidents. Since then the simplified models have an importance not only in understanding the vehicle dynamic but also in vehicle safety. A considerable amount of research has done using these linearized models in order to predict the dynamic behavior of the vehicle.

Due to the importance of vehicle models in the automotive industry throughout its history and observed the narrow use of these still in the design, development and vehicle safety.

This work developed two linear models using MATLAB/SIMULINK (bicycle model and 3 DOF) to obtain the lateral acceleration, yaw rate and roll angle, roll angle in 3 DOF model only, and compared this results with the multibody model that was simulated at MSC/ADAMS, with four different lateral accelerations (0.15, 0.35, 0.50 and 0.8 g).

The multibody model was correlated with tests held on test track in two different conditions: quasi steady state (High G) and transient limit maneuver (J Turn)

VEHICLE MODELS

Bicycle Model

The coordinate system used to develop the bicycle model is shown in “Fig.1”. It is possible to see that the side slip angle is represented in relation to the center of gravity of the vehicle. This is not always made in the development of this kind of model. However, it is extremely important since it has the same vehicle has different side slip angles at different points. (Horcaio, 2013).

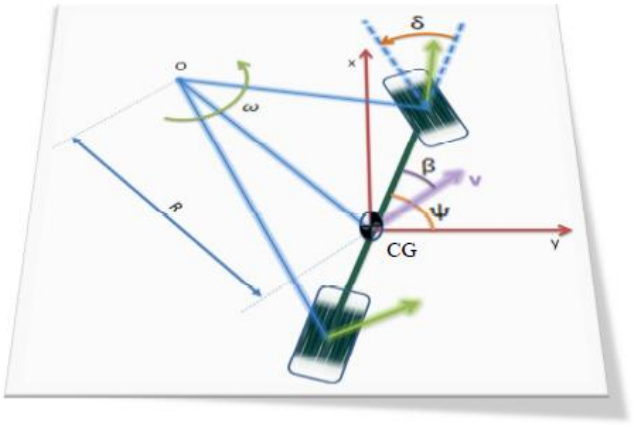

Figure 1 – Bicycle Model

In this model, the longitudinal forces and normal load as well as variations in tire will be not considered. Another consideration about this model in relation to the height of the center of gravity, which is located at a height equal to zero.

To the bicycle model equations to compute $\dot{\beta}$ and $\ddot{\psi}$ are:

$$\dot{\beta} = \frac{C_{sf}}{m.v}.\left(-\delta - \beta + \frac{l_f.\dot{\psi}}{v}\right) + \frac{C_{sr}}{m.v}.\left(-\beta - \frac{l_r.\dot{\psi}}{v}\right) + \dot{\psi} \tag{1}$$

$$\ddot{\psi} = \frac{C_{sf}.l_f}{I_{zz}}.\left(\delta + \beta - \frac{l_f.\dot{\psi}}{v}\right) - \frac{C_{sr}.l_r}{I_{zz}}.\left(\beta + \frac{l_r.\dot{\psi}}{v}\right) \tag{2}$$

Or

$$\begin{bmatrix}\dot{\beta}\\ \ddot{\psi}\end{bmatrix} = \begin{bmatrix}\frac{-C_{sf}-C_{sr}}{m.v} & \frac{C_{sf}.l_f - C_{sr}.l_r}{m.v^2} + \frac{v}{v}\\ \frac{C_{sf}.l_f - C_{sr}.l_r}{I_{zz}} & \frac{-C_{sf}.{l_f}^2 - C_{sr}.{l_r}^2}{I_{zz}.v}\end{bmatrix}\begin{bmatrix}\beta\\ \dot{\psi}\end{bmatrix} + \begin{bmatrix}-\frac{C_{sf}}{m.v}\\ \frac{C_{sf}.l_f}{I_{zz}}\end{bmatrix}[\delta] \tag{3}$$

3 D.O.F. Model

In the “Fig. 2” is showed the 3 D.O.F. model. All the equations are developed in (Horcaio, 2013).

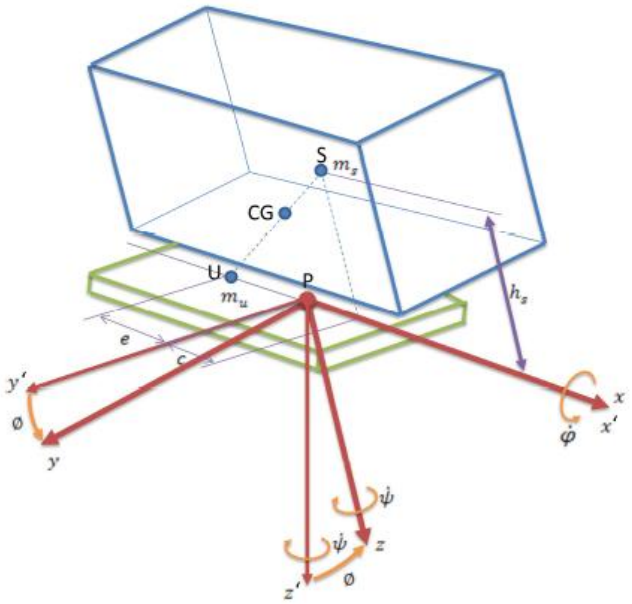

Figure 2 – 3 DOF model

Writing the equation to this model in matrix form:

$$\begin{bmatrix} \ddot{\varphi} \\ \dot{\beta} \\ \dot{\varphi} \\ \ddot{\psi} \end{bmatrix} = \begin{bmatrix} a_{11} & a_{12} & a_{13} & a_{14} \\ a_{21} & a_{22} & a_{23} & a_{24} \\ a_{31} & a_{32} & a_{33} & a_{34} \\ a_{41} & a_{42} & a_{43} & a_{44} \end{bmatrix} \begin{bmatrix} \dot{\varphi} \\ \beta \\ \varphi \\ \dot{\psi} \end{bmatrix} + \begin{bmatrix} b_{11} \\ b_{21} \\ b_{31} \\ b_{41} \end{bmatrix} [\delta] \tag{4}$$

Where

$$a_{11} = \frac{m.I_z.L_p}{m.I_x.I_z - m_s{}^2.h_s{}^2.I_z - m.I_{zx}{}^2} \tag{5}$$

$$a_{12} = \frac{-I_z.m_s.h_s.Y_\beta - I_{zx}.m.N_\beta}{m.I_x.I_z - m_s{}^2.h_s{}^2.I_z - m.I_{zx}{}^2} \tag{6}$$

$$a_{13} = \frac{I_z.m.L_\emptyset - m_s.I_z.h_s.Y_\emptyset - m.I_{zx}.N_\emptyset}{m.I_x.I_z - m_s{}^2.h_s{}^2.I_z - m.I_{zx}{}^2} \tag{7}$$

$$a_{14} = \frac{-m_s.h_s.I_z.Y_r - m.I_{zx}.N_r}{m.I_x.I_z - m_s{}^2.h_s{}^2.I_z - m.I_{zx}{}^2} \tag{8}$$

$$a_{21} = \frac{-m_s.h_s.I_z.L_p}{v.\left(m.I_x.I_z - m_s{}^2.h_s{}^2.I_z - m.I_{zx}{}^2\right)} \tag{9}$$

$$a_{22} = \frac{\left(I_x.I_z - I_{zx}{}^2\right).Y_\beta + I_{zx}.m_s.h_s.N_\beta}{v.\left(m.I_x.I_z - m_s{}^2.h_s{}^2.I_z - m.I_{zx}{}^2\right)} \tag{10}$$

$$a_{23} = \frac{-I_z.m_s.h_s.L_\emptyset + \left(I_x.I_z - {I_{zx}}^2\right).Y_\emptyset + m_s.I_{zx}.h_s.N_\emptyset}{v.\left(m.I_x.I_z - {m_s}^2.{h_s}^2.I_z - m.{I_{zx}}^2\right)} \quad (11)$$

$$a_{24} = \frac{\left(I_x.I_z - {I_{zx}}^2\right).Y_r + m_s.h_s.I_{zx}.N_r}{v.\left(m.I_x.I_z - {m_s}^2.{h_s}^2.I_z - m.{I_{zx}}^2\right)} - 1 \quad (12)$$

$$a_{31} = 1$$

$$a_{32} = 0$$

$$a_{33} = 0$$

$$a_{34} = 0$$

$$a_{41} = \frac{-m.I_{zx}.L_p}{m.I_x.I_z - {m_s}^2.{h_s}^2.I_z - m.{I_{zx}}^2} \quad (13)$$

$$a_{42} = \frac{I_{zx}.m_s.h_s.Y_\beta + \left(I_x.m - {m_s}^2.{h_s}^2\right).N_\beta}{m.I_x.I_z - {m_s}^2.{h_s}^2.I_z - m.{I_{zx}}^2} \quad (14)$$

$$a_{43} = \frac{-I_{zx}.m.L_\emptyset + m_s.I_{zx}.h_s.Y_\emptyset + \left(I_x.m - {m_s}^2.{h_s}^2\right).N_\emptyset}{m.I_x.I_z - {m_s}^2.{h_s}^2.I_z - m.{I_{zx}}^2} \quad (15)$$

$$a_{44} = \frac{m_s.h_s.I_{zx}.Y_r + \left(I_x.m - {m_s}^2.{h_s}^2\right).N_r}{m.I_x.I_z - {m_s}^2.{h_s}^2.I_z - m.{I_{zx}}^2} \quad (16)$$

$$b_{11} = \frac{-I_z.m_s.h_s.Y_\delta - m.I_{zx}.N_\delta}{m.I_x.I_z - {m_s}^2.{h_s}^2.I_z - m.{I_{zx}}^2} \quad (17)$$

$$b_{21} = \frac{\left(I_x.I_z - {I_{zx}}^2\right).Y_\delta + I_{zx}.m_s.h_s.N_\delta}{v.\left(m.I_x.I_z - {m_s}^2.{h_s}^2.I_z - m.{I_{zx}}^2\right)} \quad (18)$$

$$b_{31} = 0$$

$$b_{41} = \frac{I_{zx}.m_s.h_s.Y_\delta + \left(I_x.m - {m_s}^2.{h_s}^2\right).N_\delta}{m.I_x.I_z - {m_s}^2.{h_s}^2.I_z - m.{I_{zx}}^2} \quad (19)$$

Multibody Model

The vehicle chosen for this work was a SUV, due to its characteristics are the most favorable for the roll angle analysis because this type of vehicle has higher center of gravity than urban compact vehicles.

The characteristics of the vehicle are in "Tab. 1" and the multibody model was simulated using MSC/ADAMS software. The tires used in this model are the same in front and in rear axles of the vehicle. The compliance was not considered in this simulation.

Table 1 – Characteristics of the vehicle.

Properties	Value
Total vehicle mass (kg)	1468,5
Mass front axle (kg)	814,8
Mass rear axle (kg)	653,7
Unsprung mass front axle (kg)	79,3
Unsprung mass rear axle (kg)	75,7
C.G. height (mm)	644
Wheelbase (mm)	2522
Yaw inertia moment (kg.m^2)	2453
Roll inertia moment (kg.m^2)	591
Inertia product yaw/roll (kg.m^2)	87
Lateral tire stick coefficient (N/degree)	1103
Front steering due to roll (degree/degree)	0.0402

Rear steering due to roll (degree/degree)	-0.0225
Front camber variation (degree/degree)	-0.79
Rear camber variation (degree/degree)	-0.48
Front Damping (Nms/rad)	2683.8
Rear Damping (Nms/rad)	2062.8
Front roll stiffness (N/m)	63020.1
Rear roll stiffness (N/m)	43579.9
Front spring rate (N/mm)	20.2
Rear spring rate (N/mm)	21
Roll center to C.G. height (m)	0.528
Wheel steering ratio (degree/degree)	16.57

CORRELATION BEETWEN MULTIBODY MODEL AND EXPERIMENTAL RESULTS

Multibody model was correlated with real vehicle in two different maneuvers, the High-G and J turn with 90 degrees in steering wheel. The High-G maneuvers consists in to keep the longitudinal speed of the vehicle constant at 75 km/h and apply a steering angle in one constant rate until 90 degrees in steering wheel, as can be seen in "Fig. 3 (a)". The J turn maneuver is one test where the driver turn steering wheel 90 degrees quickly, keep the steering wheel at this position during five seconds and after this time, return the steering wheel 90 degrees "Fig. 4 (a)". The longitudinal speed of J turn is 100 km/h and it generated 0.8 g of lateral acceleration with 90 degrees of steering. The first maneuver is considered one quasi steady state condition, but the second is considered a limit transient maneuver.

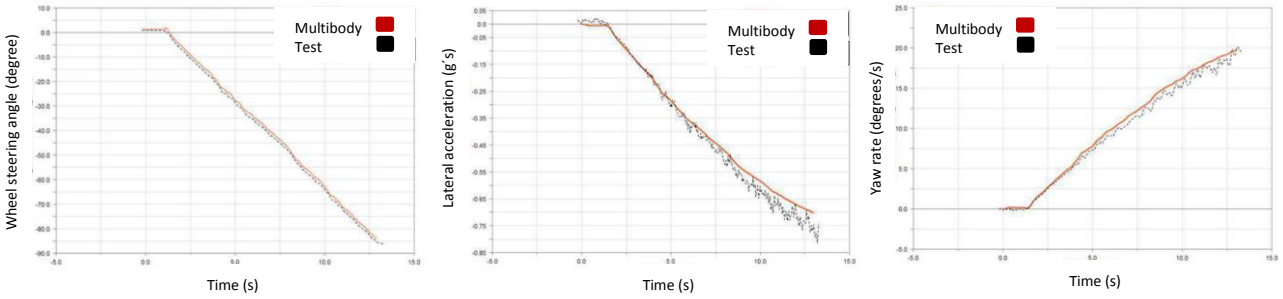

(a) (b) (c)

Figure 3 – Correlation of results of track test and multibody model to high G maneuver

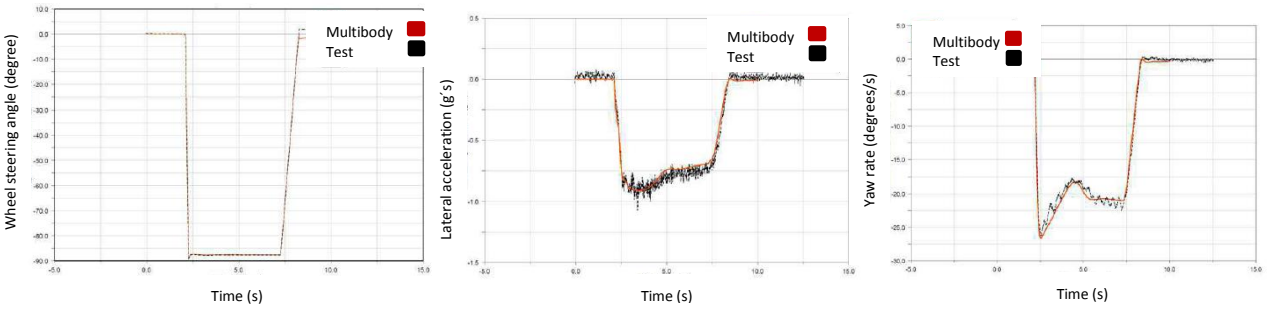

(a) (b) (c)

Figure 4 – Correlation of results of track test and multibody model to J turn maneuver

In "Fig. 3 (b)" and "Fig. 3 (c)" and in "Fig. 4 (b)" and "Fig. 4 (c)" are showing the good correlation between multibody model and tests of real vehicle in lateral acceleration and yaw rate. So, is possible to use the multibody model to simulate and compare the results of this model with the maneuvers in the bicycle model and 3 DOF model.

Figure 5 and Figure 6 shows the body displacement during high G and J turn maneuvers respectively. This body displacement was measured with linear variable displacement transducer in the shock absorber. In these figures is possible to see again the good correlation between test and multibody model. This information is import to identify any change during the vehicle behavior and identify any error in simulation parameters.

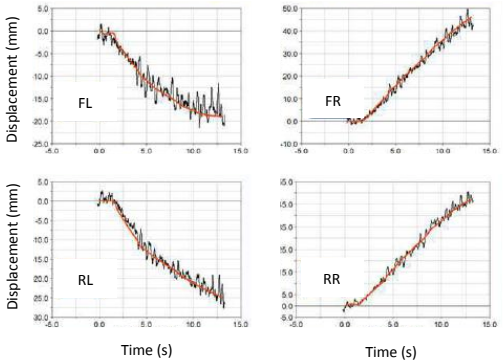

Figure 5 – Body displacement correlation during High G test

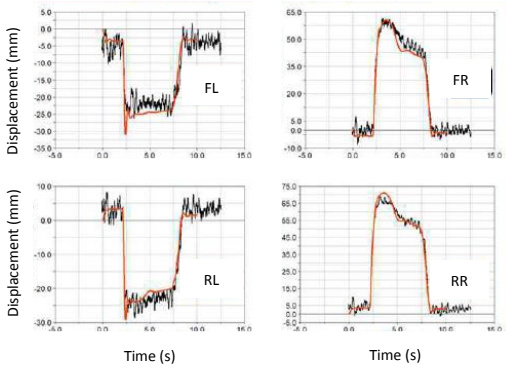

Figure 6 – Body displacement correlation during J turn test

Simplified Models

The model of three degrees of freedom is nothing more than a bicycle model with the addition of body rolling due to CG height. So, is expected that both models show the same results to lateral acceleration and yaw rate, when the height of the CG of the vehicle is zero in the model of three degrees of freedom. In order to confirm this statement, both models were tested in same condition to generate 0.5 g of lateral acceleration and the results for these two models are showed in the "Fig. 7".

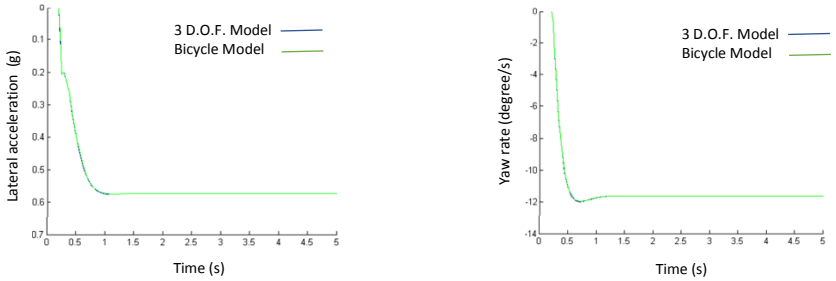

Figure 7 – Bicycle model and 3 DOF model

Figure 8 shows the difference between the results of these two models when the CG`s height is inputted in the 3 DOF model. The C.G. height reduced lateral acceleration and yaw ratio due to body rolling and the bicycle model shows its limitations due to center of gravity is on the plane.

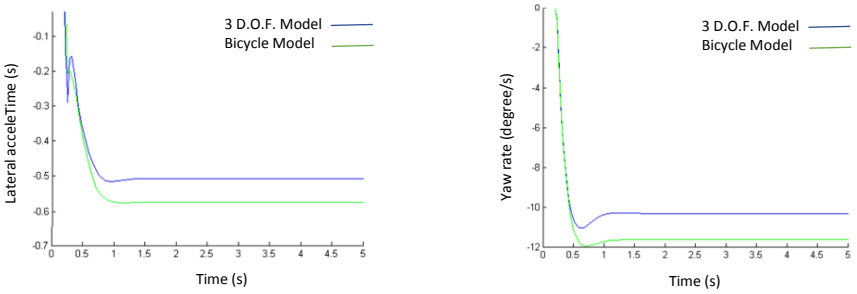

Figure 8 – Bicycle model and 3 DOF model with CG height inputted

Multibody model Compared with Simplified Models

Four different steering angle was used in the multibody model to generated four different lateral accelerations. These lateral accelerations were 0.15, 0.35, 0.5 and 0.8 g. All simulations were computed with longitudinal speed of 100 km/h.

These values were chosen because they represent different conditions in the vehicle behavior. The 0.15 g is one linear condition of the vehicle, 0.35 and 0.5 g were used because they are values always found in the literature as acceptable to linear models and 0.8 g is a limit condition for this kind of vehicle.

In the "Fig. 9" are the results of lateral acceleration (a) and yaw rate (b) to multibody model and bicycle model. Multibody model shows lateral acceleration of 0.15 g but bicycle model shows the lateral acceleration of 0.25 g, even this region being a linear region of the tire. In the "Fig. 9 (b)", yaw rate shows the difference in the results for these models.

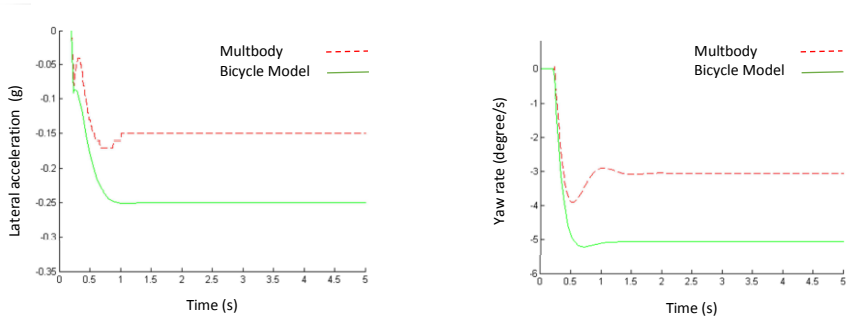

(a) (b)

Figure 9 – Bicycle model compared with multibody model 0.15 g

The lateral acceleration, "Fig. 10 (a)", and yaw rate "Fig. 10 (b)"were compared between multibody model and 3 DOF model. Both results to 3 DOF were better than bicycle model, but even in this linear region, the difference is very large.

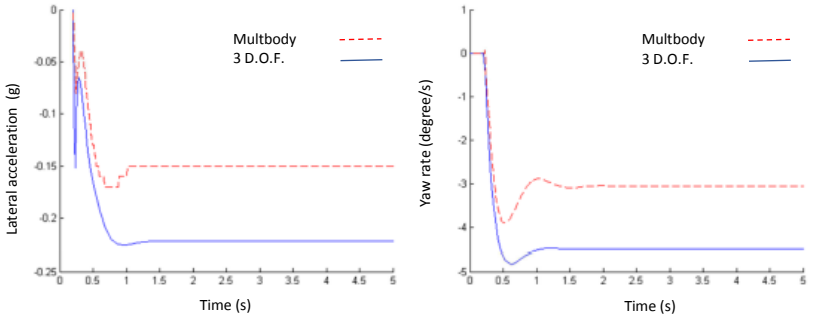

(a) (b)

Figure 10 – 3 D.O.F. model compared with multibody model 0.15 g

Figure 11 is showing the rolling angle. The results difference between 3 DOF and multibody in this case is less than the difference to lateral acceleration and yaw rate. This happened because rolling angle is related to the mass and inertia, so, it does not suffer influence of nonlinear parameters of the model.

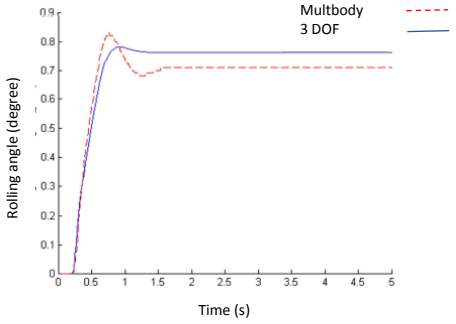

Figure 11 – 3 D.O.F. model compared with multibody model 0.50 g

With condition to generate lateral accelerations of 0.35 and 0.5 g, the results difference in rolling angle keeps acceptable between 3 DOF model and multibody model, but the difference between lateral acceleration and yaw rate results increased to unacceptable levels.

With lateral acceleration of 0.8 g even the results difference between rolling angle in these two models were very large as showed in the "Fig. 12". This difference occur due to multibody model has a polymer spring that limits body rolling but in the 3 DOF model spring has linear spring rates without body rolling limits.

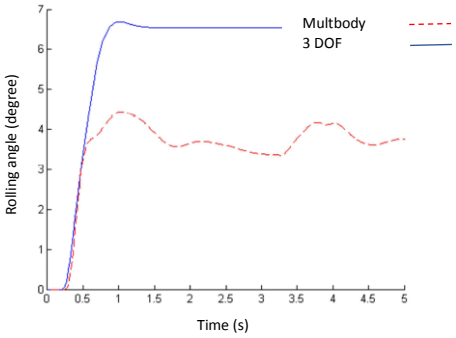

Figure 12 – 3 D.O.F. model compared with multibody model 0.80 g

CONCLUSIONS

Two linear models very used in automotive industries were implemented using MATLAB/SIMULINK.

One multibody model was implemented using MSC/ADAMS and the simulation results of this model were compared with experimental results in two different maneuvers held on test track. The test's results demonstrated that the multibody model and vehicle had good correlation.

Four different wheel steering angle were inputted into the models to generate four levels of lateral acceleration (0.15, 0.35, 0.50 and 0.8 g).

The linear models do not have good correlation with the multibody model even to low values of lateral acceleration. Region where these models normally are applied.

The rolling angle in the 3 DOF model keep good correlation with the multibody model up to 0.5 g of lateral acceleration, but with 0.8 g the variation of results were large due to limitations of the spring model.

ACKNOWLEDGMENTS

The authors acknowledge University Center of FEI and Ford Motor Company.

REFERENCES

Abe, Masato; MANNING, Warren. Vehicle Handling Dynamics: Theory and Application. Amsterdam: Butterworth-Heinemann, 2009.

Andersson, Johan. Vehicle Dynamics - optimization of Electronic Stability Program for sports cars. 2008. Master Thesis - Luleå University of Technology, Department of Applied Physics and Mechanical Engineering – division of Computer Aided Design, 2008.

Barak, Pinhas; Tianbing, Sun. On Body Roll Angle during Transient Response Maneuver of a 3-D Model. SAE Technical Paper Series 2003-01-0963, Detroit, Michigan, mar. 2003.

Duarte, Murilo. Simulação de Ride Primário e Secundário através de Carregamento de Pista. 2010. 126 f. Master Thesis Escola de Engenharia São Carlos, Universidade de São Paulo, São Carlos, 28 out. 2010.

Fernandes, Claudio; Duarte, Murilo. Archetypal vehicle dynamics model for resistance rollover prediction. SAE Technical Paper Series 2010-01-0715, Detroit, Michigan, 2010.

Horcaio, Jean Tavares. Dinâmica veicular: análise das respostas dos modelos de bicicleta, três graus de liberdade e multicorpos comparados com experimentos em pista e determinação dos seus limites de utilização, Master Thesis, Centro Universitário da FEI, 2013.

Milliken, William F.; Milliken, Douglas L. Race Car Vehicle Dynamics. Pennsylvania: SAE International, 1995.

Segel, Leonard. Theoretical Prediction and Experimental Substantiation of the Response of the Automobile to Steering Control, 30 Ago.1956

RESPONSIBILITY NOTICE

The authors are the only responsible for the material included in this paper.